

Review

Critical Review of $\text{Ca}(\text{OH})_2/\text{CaO}$ Thermochemical Energy Storage Materials

Yupeng Feng ¹, Xuhan Li ², Haowen Wu ¹, Chaoran Li ¹, Man Zhang ¹ and Hairui Yang ^{1,*}

¹ State Key Laboratory of Power System and Generation Equipment, Department of Energy and Power Engineering, Tsinghua University, Beijing 100084, China

² School of Energy Science and Engineering, Harbin Institute of Technology, Harbin 150001, China

* Correspondence: yhr@mail.tsinghua.edu.cn

Abstract: Thermal energy storage is an essential technology for improving the utilization rate of solar energy and the energy efficiency of industrial processes. Heat storage and release by the dehydration and rehydration of $\text{Ca}(\text{OH})_2$ are hot topics in thermochemical heat storage. Previous studies have described different methods for improving the thermodynamic, kinetic, and structural stability of $\text{Ca}(\text{OH})_2$ to improve energy storage density, energy storage rate, and cycle stability, respectively. Here, the mechanisms and effects of different techniques on the performance improvement of $\text{Ca}(\text{OH})_2$ and some common problems were reviewed. Specific problems were also clarified based on the characteristics of different technologies. Finally, suggestions for the future development of $\text{Ca}(\text{OH})_2$ heat storage materials were provided.

Keywords: $\text{Ca}(\text{OH})_2$; CaO ; thermochemical heat storage; material improvement

1. Introduction

The extensive use of fossil fuels has resulted in greenhouse gas emissions and environmental pollution. In response, the global energy sector is transitioning from fossil energy to renewable energy to achieve the goal of low carbon emissions and green development. The International Energy Agency (IEA) predicts that by 2050, 90% of electricity will be generated from renewable energy sources, with solar energy being the largest source [1]. However, renewable energy is characterized by intermittency and volatility. Furthermore, when a power system is dominated by renewable energy, there is a mismatch between energy supply and demand in time and space. This poses a significant challenge to the expansion of renewable energy in power systems and necessitates the development of new power systems [2,3]. Energy storage technology is an essential component of new renewable energy power systems. In particular, this study focused on thermal energy storage technology.

Thermal energy storage technology is a large-scale energy storage technology with ecological and cost efficiency that can realize the direct storage of thermal energy [4] as well as the indirect storage of electrical energy [5,6]. Compared with electrical batteries, thermal energy storage can achieve gigawatt-hour-scale energy storage at a lower cost [7]. Furthermore, compared with pumped hydro energy storage, thermal energy storage has more compact storage volumes. The application scenarios of thermal energy storage mainly include concentrated solar power generation and waste heat recovery of industrial processes, which help achieve continuous and stable all-weather operation of solar thermal power generation and improve the energy efficiency of industrial systems [8–11]. Thermal energy storage includes sensible, latent, and thermochemical heat storage. Sensible and latent heat storage uses temperature changes and phase transitions to achieve heat storage and release [12], whereas thermochemical heat storage uses reversible chemical reactions (mainly gas–solid reactions) to achieve heat storage and release [13]. Thermochemical heat storage has the



Citation: Feng, Y.; Li, X.; Wu, H.; Li, C.; Zhang, M.; Yang, H. Critical Review of $\text{Ca}(\text{OH})_2/\text{CaO}$ Thermochemical Energy Storage Materials. *Energies* **2023**, *16*, 3019. <https://doi.org/10.3390/en16073019>

Academic Editor: James Klausner

Received: 29 January 2023

Revised: 12 March 2023

Accepted: 22 March 2023

Published: 25 March 2023



Copyright: © 2023 by the authors. Licensee MDPI, Basel, Switzerland. This article is an open access article distributed under the terms and conditions of the Creative Commons Attribution (CC BY) license (<https://creativecommons.org/licenses/by/4.0/>).

advantages of high energy storage density (0.5–3 GJ/m³), wide operating temperatures, and long-term energy storage [14–16], making it a major focus of research [17].

Among the many thermochemical heat storage materials, Ca(OH)₂ is among the most promising owing to the reversible reaction of Ca(OH)₂ dehydration and CaO hydration [18,19]. This material has the advantages of low cost, high energy storage density, good reversibility, cycle stability, nontoxicity, and fast reaction kinetics [20]. The working principle of this approach is shown in Equation (1) and Figure 1. During heat storage, Ca(OH)₂ absorbs heat and decomposes to produce CaO and steam, storing the heat as chemical energy. In the exothermic process, CaO reacts with steam to form Ca(OH)₂, releasing stored chemical energy as heat. Under atmospheric pressure, the heat storage temperature of Ca(OH)₂ ranges from 400 to 600 °C, and the heat release temperature ranges from 25 °C to approximately 500 °C (as determined from the partial pressure of the steam involved in the reaction) [21]. These temperatures enable the integration of this heat storage system with the steam Rankine cycle while allowing flexible adjustment of the heat storage and release power by controlling the heat input and partial steam pressure.

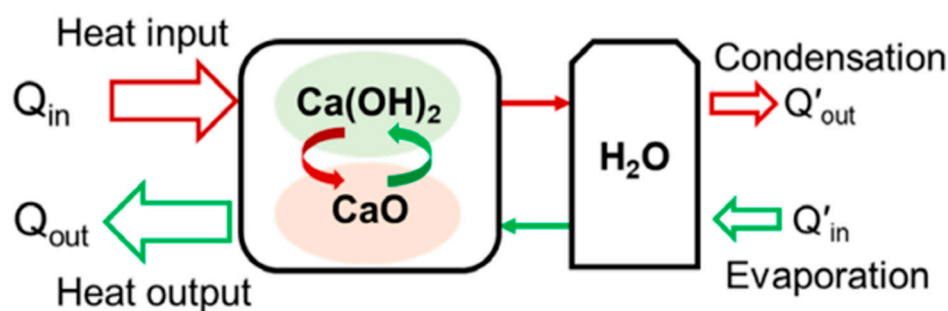


Figure 1. Thermochemical heat storage schematic diagram depicting Ca(OH)₂ dehydration and CaO hydration. (Reprinted with permission from ref. [22]. Copyright 2021 John Wiley & Sons).

The Ca(OH)₂/CaO thermochemical heat storage system mainly comprises a heat storage material and a reactor; therefore, development of a more efficient heat storage system should first focus on improving the heat storage material and optimizing the reactor [12]. This study focuses on improving Ca(OH)₂/CaO heat storage materials. Although the theoretical energy storage density of Ca(OH)₂ can reach 1400 kJ/kg or 3.1 GJ/m³, the actual volumetric storage density is approximately two-fold lower than the theoretical value because of its low apparent density [23]. From the perspective of energy storage rates, a lower thermal conductivity (approximately 0.1 W/m·K) limits the heat transfer rate of the material and thus the reaction rate. In terms of cycle stability, the agglomeration and fragmentation of Ca(OH)₂ particles after multiple cycles deteriorate the mass transfer effect and reduce the reaction rate, which is not conducive to practical applications. Additionally, the high decomposition temperature of Ca(OH)₂ (approximately 350 °C) limits the types of heat sources that can be matched. Therefore, the thermodynamic properties, kinetic properties, and structural stability of Ca(OH)₂ must be optimized to improve its energy storage density, energy storage rate, and cycle stability.

Since Wentworth and Chen [13] first demonstrated that Ca(OH)₂/CaO could be used for heat storage in 1976, this material has been the subject of considerable research for more than 40 years. Material improvement accounts for a large proportion of existing studies, enabling continuous improvements in the performance of Ca(OH)₂ to aid in the rapid transformation of the current energy system. Yuan et al. [24] summarized the application of CaO-based materials and the role of CaO/Ca(OH)₂ cycles, CaO/CaCO₃ cycles, and the coupling of CaO/Ca(OH)₂ and CaO/CaCO₃ cycles in thermochemical heat storage. Yuan et al. focused on the process and influence of key variables (such as temperature, vapor pressure, and CO₂) and described the improvement effect of four additives (Al₂O₃,

LiOH, Na₂Si₃O₇, and nano-SiO₂) on the heat storage materials. Wang et al. [25] summarized research on the physical and chemical properties of Ca(OH)₂ (such as specific heat capacity, reaction enthalpy, chemical equilibrium, and kinetics), highlighted current problems in the application of this material (high decomposition temperature, low thermal conductivity, agglomeration, cracking, and carbonation) and solutions, and introduced current application fields. However, a comprehensive review on improving Ca(OH)₂ materials is lacking. Considering the importance of this research direction, this review summarized the research on material improvement from a technical perspective. The mechanisms and effects of different technologies on the performance improvement of Ca(OH)₂ heat storage materials were reviewed, existing problems were discussed, and suggestions for future development were provided. Different reactors require different heat storage materials, that is, powder or granulated materials. Therefore, Ca(OH)₂/CaO heat storage materials were reviewed herein based on this characteristic. Different performance enhancement techniques are available for powders and granulation materials, as shown in Figure 2. Notably, powder materials can be improved by doping modifications, composite powders, surface coatings, and supporting frames technologies, while granulated materials can be improved using composite granules, surface coatings, binder matrices, and macro-encapsulation technologies.

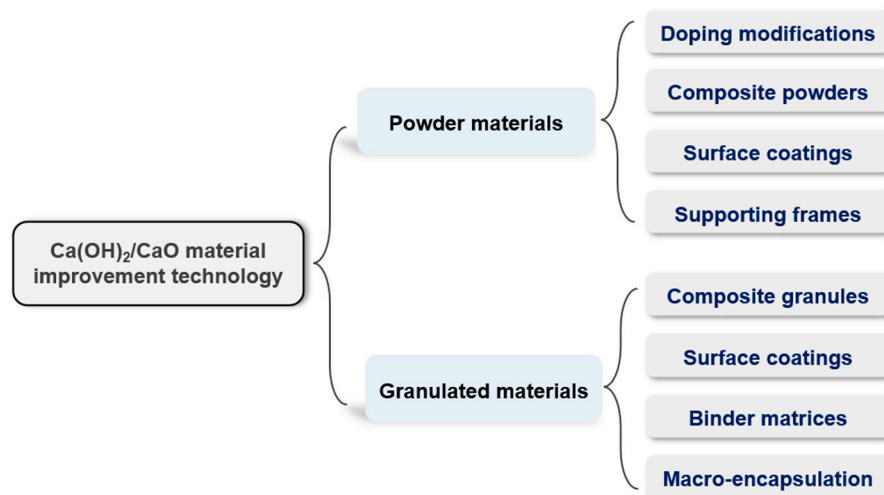


Figure 2. Classification of material performance enhancement techniques.

2. Performance-Improvement Technology for Powder Materials

2.1. Doping Modifications

Murthy et al. [26] prepared Ca(OH)₂ doped with 1, 3, and 5 wt.% Al, Ni, and Zn using the co-precipitation method, finding that the dopants decreased the dehydration temperature of Ca(OH)₂ and increased the reaction rate. In particular, Al had the best effect at the same doping level. Two mechanisms were proposed for this effect: first, the addition of Ni, Al, and Zn induces crystal defects and forms potential nucleation sites, thereby increasing the number of interfacial propagating nuclei; second, elemental doping creates energetic centers and reduces the activation energy in some steps of the chemical transformation. By comparing the decomposition temperatures of the doped samples obtained via the co-precipitation method and the mixed samples obtained via direct mixing, the authors found that these two preparation methods had almost the same effect on reducing the decomposition temperature of Ca(OH)₂. Therefore, if the objective is only to reduce the decomposition temperature, the direct mixing method can replace the expensive co-precipitation method.

Yan and Zhao [27] used the first principles method and transition state theory to study the mechanism of separate Li and Mg doping in Ca(OH)₂ thermochemical heat storage at the microscopic level. The influence of doping on the macroscopic heat storage process

was determined by comparing the transition state, energy barrier, and density of electronic states of the undoped and doped systems. Their theoretical calculation results showed that Li doping could reduce the energy barrier of the $\text{Ca}(\text{OH})_2$ dehydration reaction from 0.40 eV to 0.11 eV, which means that Li-doped samples completed the dehydration reaction at a lower temperature. Analysis of the pseudogap width in the density of electronic states revealed that the pseudogap width was reduced by Li doping, thus reducing the bond energy; that is, at the same temperature, Li doping caused the O-H and OH-Ca bonds of $\text{Ca}(\text{OH})_2$ to break more quickly, which increased the dehydration rate. In comparison, the Mg doping had little effect on the decomposition of $\text{Ca}(\text{OH})_2$. Based on theoretical research, Yan and Zhao [28] prepared samples with different Li/Ca molar ratios (2%, 5%, 10%, and 30%) using the ball milling method and confirmed this phenomenon through thermogravimetric experiments. As shown in Figure 3, with increased Li doping, the time required to dehydrate $\text{Ca}(\text{OH})_2$ was shortened and the heat storage rate constantly increased. However, it is worth noting that a conversion of 0.3 was used as the demarcation point in the kinetic process of Li-doped $\text{Ca}(\text{OH})_2$ decomposition, and the two stages conform to different kinetic mechanism functions. Yan and Zhao [28] suggested that the reason for this phenomenon is that different effects are produced when the distance between the atoms in the $\text{Ca}(\text{OH})_2$ crystal and Li atoms exceeds a specific limit. Notably, Li doping had little effect on the heat storage capacity (including the reaction enthalpy and specific heat capacity) of $\text{Ca}(\text{OH})_2$.

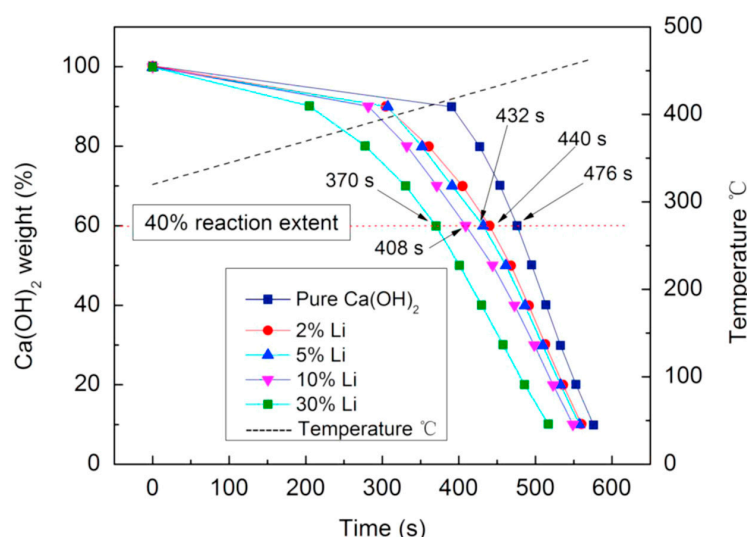


Figure 3. Decomposition of $\text{Ca}(\text{OH})_2$ doped with different amounts of Li at a heating rate of $15\text{ }^\circ\text{C}/\text{min}$. (Reprinted with permission from ref. [28]. Copyright 2015 Elsevier).

Shkatulov and Aristov [29] screened the chlorides, nitrates, sulfates, and acetates of alkaline metals (Li, Na, and K), which reduced the dehydration temperature and increased the dehydration rate of $\text{Ca}(\text{OH})_2$. As shown in Figure 4, 5 wt.% KNO_3 doping yielded the best results, reducing the dehydration temperature of $\text{Ca}(\text{OH})_2$ by approximately $40\text{ }^\circ\text{C}$, and the heat storage density was 94.8% of that of pure $\text{Ca}(\text{OH})_2$. At $390\text{ }^\circ\text{C}$ and a partial steam pressure of 24 mbar, the heat storage rate of $\text{Ca}(\text{OH})_2$ was increased 4.6-fold, the average heat storage power was $365 \pm 15\text{ W/kg}$, and complete reversibility was achieved over five cycles. Based on infrared spectroscopy, Shkatulov and Aristov [23] suggested that the insertion of nitrate ions into the $\text{Ca}(\text{OH})_2$ lattice causes the collapse of the KNO_3 crystalline structure, lowers the symmetry of the nitrate ions, and creates additional structural defects, which can further promote nucleation and accelerate dehydration. Wang et al. [30] prepared $\text{Ca}(\text{OH})_2$ composites containing KNO_3 using mechanical and solution mixing methods and observed similar phenomena. Based on kinetic analysis and morphological observations, the authors showed that KNO_3 could reduce the apparent activation energy

of $\text{Ca}(\text{OH})_2$ decomposition and regulate the morphology of $\text{Ca}(\text{OH})_2$ to enhance the mass transfer effect.

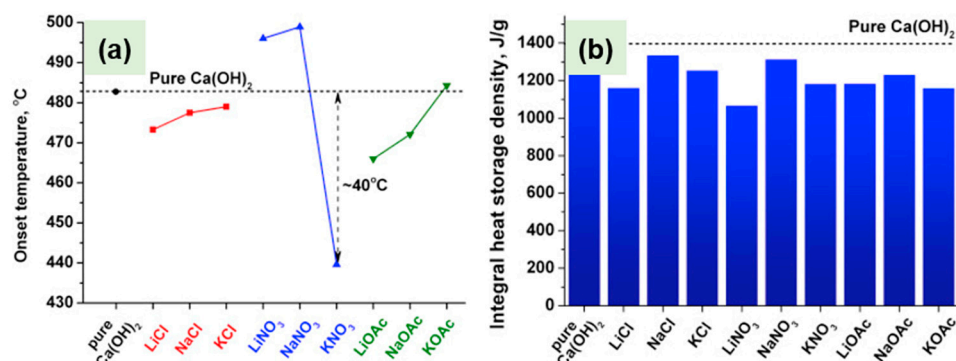


Figure 4. The effect of adding different salts on $\text{Ca}(\text{OH})_2$: (a) dehydration onset temperature and (b) heat storage density of “salt/ $\text{Ca}(\text{OH})_2$ ”. (Reprinted with permission from ref. [29]. Copyright 2015 Elsevier).

Maruyama et al. [31] prepared samples containing lithium compounds (LiOH , LiCl , and Li_2CO_3) using an impregnation method with both single and co-doping. The peak dehydration temperatures of $\text{Ca}(\text{OH})_2/\text{LiOH}/\text{LiCl} = 100:5:5$ and $\text{Ca}(\text{OH})_2/\text{LiCl}/\text{Li}_2\text{CO}_3 = 100:10:5$ (molar ratios) were approximately 60 °C lower than that of pure $\text{Ca}(\text{OH})_2$. This indicates that the co-addition of Li compounds renders $\text{Ca}(\text{OH})_2$ heat storage suitable for low-temperature heat sources. Based on the X-ray diffraction (XRD) patterns and crystal lattice information, Maruyama et al. [31] suggested that the doped Li^+ was located in the interlayer of the $\text{Ca}(\text{OH})_2$ crystal structure (Figure 5), which increased the lattice volume of $\text{Ca}(\text{OH})_2$ and rendered the crystal fragile, thereby promoting dehydration. It is worth noting that LiCl reacts with $\text{Ca}(\text{OH})_2$ to form $\text{CaCl}(\text{OH})$ during the preparation process, which inhibits dehydration at high temperatures.

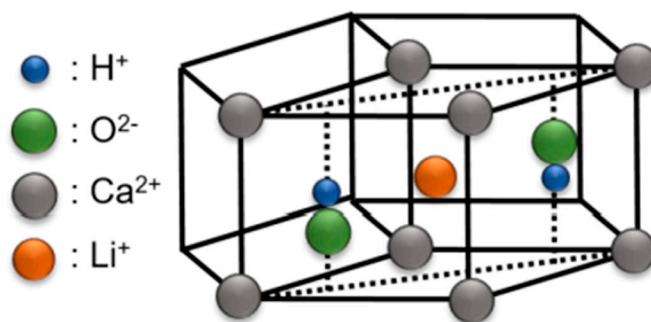


Figure 5. Schematic diagram of Li-doped $\text{Ca}(\text{OH})_2$ crystal structure. (Reprinted with permission from ref. [31]. Copyright 2020 American Chemical Society).

Bian et al. [32] prepared Ce- and Mn-doped CaO using a wet mixing method in which the mass ratios of CeO_2/CaO and MnO_2/CaO were 10:90 and 1.2:100, respectively. After 10 cycles, the hydration conversion of Mn-doped CaO was 88.4%, which was 1.06-fold higher than that of Ce-doped CaO and 1.12-fold higher than that of CaO . Density functional theory calculations showed that Mn and Ce doping accelerated H_2O adsorption on the CaO surface. As shown in Figure 6, Mn doping reduced the energy barrier of the CaO hydration reaction by 84.3%, and this effect was greater than that of Ce doping. As a result, Mn-doped CaO showed higher hydration reactivity. The above-mentioned studies on doping modifications are summarized in Table 1.

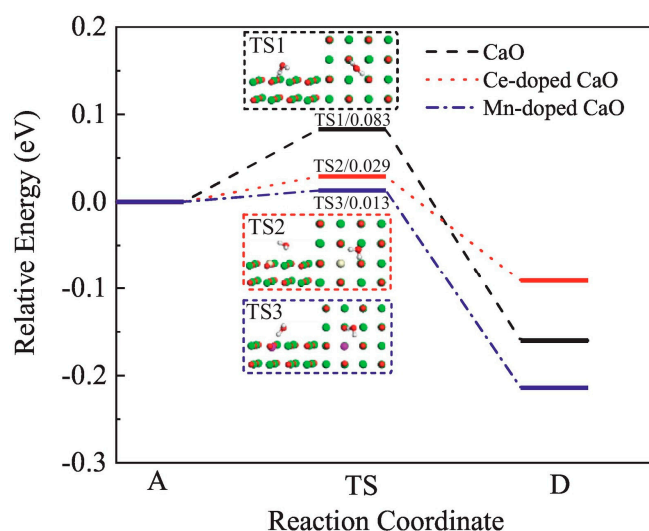


Figure 6. Relative energy of the hydration reaction process on CaO and Ce-doped and Mn-doped CaO surfaces. (Reprinted with permission from ref. [32]. Copyright 2022 Elsevier).

Table 1. Summary of research on doping modifications ¹.

Research	Dopant	Doping Method	Benefit
Murthy et al. [26]	Al, Ni, Zn	co-precipitation	<ul style="list-style-type: none"> ◇ dehydration temperature ↓ ◇ dehydration rate ↑ ◇ the effect of Al was the best at the same doping level
Yan and Zhao [28]	Li, Mg	ball milling	<ul style="list-style-type: none"> ◇ Li doping, dehydration temperature ↓ ◇ Li doping, dehydration rate ↑
Shkatulov and Aristov [23,29]	Li, Na, K	mechanical and solution mixing	<ul style="list-style-type: none"> ◇ dehydration temperature ↓ ◇ dehydration rate ↑ ◇ 5 wt.% KNO₃ doping was the best choice
Wang et al. [30]	K	mechanical and solution mixing	<ul style="list-style-type: none"> ◇ dehydration temperature ↓ ◇ dehydration rate ↑
Maruyama et al. [31]	Li	impregnation	<ul style="list-style-type: none"> ◇ Ca(OH)₂/LiOH/LiCl = 100:5:5 (molar ratios), dehydration temperature ↓ significantly ◇ Ca(OH)₂/LiCl/Li₂CO₃ = 100:10:5 (molar ratios), dehydration temperature ↓ significantly
Bian et al. [32]	Ce, Mn	wet mixing	<ul style="list-style-type: none"> ◇ Mn-doped CaO showed a higher hydration reactivity

¹ ↑ indicates an increase, and ↓ indicates a decrease.

2.2. Composite Powders

Kariya et al. [33] prepared a composite material of expanded graphite and Ca(OH)₂ using an ultrasonic crushing method in an ethanol solution, as shown in Figure 7. The higher the content of expanded graphite in the composites, the higher their reactivity. The average heat output of the composite with 11 wt.% expanded graphite was 1.76 kW/(kg material), which was twice that of pure Ca(OH)₂. Therefore, expanded graphite promoted the hydration reaction more effectively than the dehydration reaction. The addition of expanded graphite improved the thermal conductivity and porosity of the composites, thereby enhancing their heat and mass transfer effects. Considering that the dehydration reaction rate is mainly driven

by heat transfer and that the hydration reaction rate is jointly controlled by heat transfer and steam diffusion, the increase in the hydration rate is more significant.

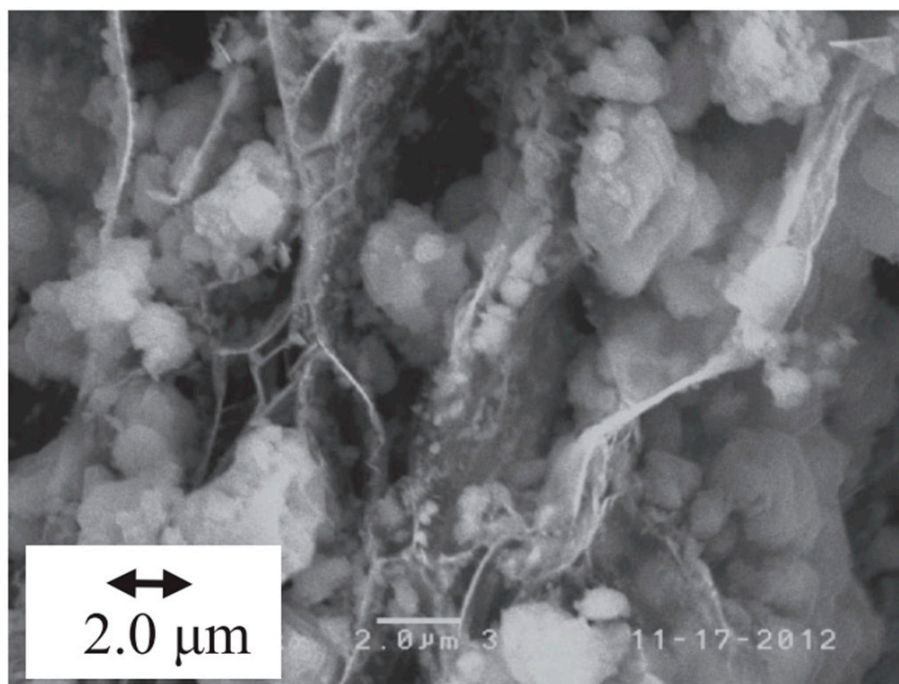


Figure 7. Microscopic images of expanded graphite/ $\text{Ca}(\text{OH})_2$ composites. (Reprinted with permission from ref. [33]. Copyright 2015 Iron and Steel Institute of Japan).

Huang et al. [34] prepared a $\text{Ca}(\text{OH})_2$ composite material with the addition of hexagonal boron nitride (HBN) using ultrasonic and magnetic agitation. The thermal conductivities of $\text{Ca}(\text{OH})_2$ at room temperature and $300\text{ }^\circ\text{C}$ improved by 13.2% and 22.9%, respectively, with 15 wt.% HBN in the composite. After 10 cycles, the heat release capacity of the composite remained at 67% (61% for pure $\text{Ca}(\text{OH})_2$), indicating good cyclic stability. HBN prevented the agglomeration of $\text{Ca}(\text{OH})_2$, and the pores formed by HBN also facilitated the diffusion of steam, contributing to a higher hydration conversion. Kinetic data further showed that adding HBN reduced the activation energy for the dehydration of $\text{Ca}(\text{OH})_2$ and increased the heat storage rate.

Li et al. [35] reported that the addition of 10 wt.% $\text{ZrO}(\text{NO}_3)_2$ could reduce the initial dehydration temperature of the composite by $61\text{ }^\circ\text{C}$. Moreover, the dehydration rate of the composite at $310\text{ }^\circ\text{C}$ was 15.7 times that of pure $\text{Ca}(\text{OH})_2$. This is because the activation energy of the dehydration of the composite was 46 kJ/mol lower than that of pure $\text{Ca}(\text{OH})_2$. The dehydration rate of the composite increased with increasing $\text{ZrO}(\text{NO}_3)_2$ addition. However, the heat storage capacity of the composite also exhibited a downward trend owing to the decrease in the $\text{Ca}(\text{OH})_2$ content in the unit mass composite. The heat storage capacity of the composite doped with 10 wt.% $\text{ZrO}(\text{NO}_3)_2$ was 75.7% of that of the pure material. To mitigate the deterioration of mass transfer caused by $\text{Ca}(\text{OH})_2$ powder agglomeration, Li et al. [35] also added carbon fibers to the composite to maintain a higher porosity and thus improve the cycle stability.

Sun et al. [36] used limestone powder and acetic acid as raw materials to obtain calcium acetate using the wet mixing method and then obtained CaO by high-temperature calcination. High hydration and dehydration conversions and cycling stability were achieved in the cyclic heat storage test. Finally, Guo et al. [22] used CaCO_3 and additives (including tetraethoxysilane, a silane coupling agent, and bis(3-triethoxysilylpropyl) pertetrasulfide) to prepare composite materials via heat treatment. Compared with pure $\text{Ca}(\text{OH})_2$, the composites containing 0.6 wt.% additives exhibited higher reactivity and more stable hydration performance under near-equilibrium conditions, which was attributed to the enhanced

effect of Ca_2SiO_4 nanoparticles on hydration reactions. Notably, when the temperature and pressure parameters are far from equilibrium or the steam partial pressure is high, the enhancement effects of the additives are insignificant because the hydration reaction of CaO is already fast under these conditions. The above-mentioned studies on composite powders are summarized in Table 2.

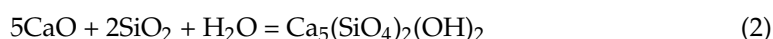
Table 2. Summary of research on composite powders ¹.

Research	Additives	Preparation Method	Benefit
Kariya et al. [33]	expanded graphite	ultrasonic crushing	<ul style="list-style-type: none"> ◇ hydration rate ↑ significantly ◇ dehydration rate ↑ ◇ thermal conductivity ↑ ◇ porosity ↑
Huang et al. [34]	hexagonal boron nitride	ultrasonic and magnetic agitation	<ul style="list-style-type: none"> ◇ thermal conductivity ↑ ◇ cycle stability ↑ ◇ dehydration rate ↑
Li et al. [35]	$\text{ZrO}(\text{NO}_3)_2$ and carbon fibers	mechanical and solution mixing	<ul style="list-style-type: none"> ◇ dehydration temperature ↓ ◇ dehydration rate ↑ ◇ porosity ↑ ◇ cycle stability ↑
Sun et al. [36]	acetic acid	wet mixing	<ul style="list-style-type: none"> ◇ dehydration conversions ↑ ◇ hydration conversions ↑ ◇ cycle stability ↑
Guo et al. [22]	tetraethoxysilane and silane coupling agent and bis(3-triethoxysilylpropyl) pertetrasulfide	heat treatment	<ul style="list-style-type: none"> ◇ higher reactivity and more stable hydration performance under near-equilibrium conditions

¹ ↑ indicates an increase, and ↓ indicates a decrease.

2.3. Surface Coatings

Roßkopf et al. [37] used magnetic agitation to deposit a small amount of nano- SiO_2 particles (with an average particle size of approximately 7 nm) on the surface of $\text{Ca}(\text{OH})_2$. The addition of small amounts (≤ 5 wt.%) of the nano- SiO_2 particles prevented the agglomeration of the $\text{Ca}(\text{OH})_2$ powder and did not inhibit the heat storage and release rate, achieving stability over eight cycles. The reduction in adhesion between the $\text{Ca}(\text{OH})_2$ particles minimized channeling effects, thus creating a more uniform flow of materials and greatly improving the flow characteristics and heat and mass transfer effects in the powder bed [38]. When studying material performance using an indirect heat transfer fixed-bed reactor, it was found that the SiO_2 coating reacted with H_2O and CaO (Equation (2)) to form reinhardbraunsite ($\text{Ca}_5(\text{SiO}_4)_2(\text{OH})_2$), which maintained the surface structural stability of the heat storage material [39]. When 10 wt.% nano- SiO_2 was added to the composite, the reinhardbraunsite accounted for approximately 30 wt.% of the composite after 10 cycles.



Xu et al. [40] studied the agglomeration behavior of $\text{Ca}(\text{OH})_2$ and CaO at the molecular level using reactive molecular dynamics simulations, as shown in Figure 8. Their results indicated that the $\text{Ca}(\text{OH})_2$ dehydration reaction was the main factor affecting material agglomeration. The effect of H_2O on the agglomeration of $\text{Ca}(\text{OH})_2$ molecules was greater than that on CaO molecules, mainly because of the different spatial displacements of the atoms during the chemical reaction. The addition of nano-silica particles to $\text{CaO}/\text{Ca}(\text{OH})_2$ effectively reduced the agglomeration rate and acted as a barrier.

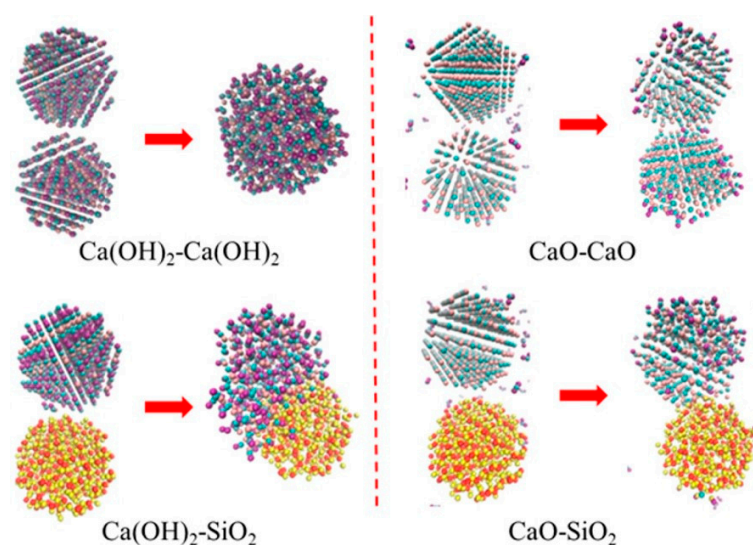


Figure 8. Effect of the addition of nano-SiO₂ on the molecular agglomeration of Ca(OH)₂ or CaO. (Reprinted with permission from ref. [40]. Copyright 2017 American Chemical Society).

Amjadi et al. [41,42] used the dry mixing method to prepare Ca(OH)₂ particles coated with hydrophilic and hydrophobic silica nanoparticles to improve fluidization. The sieve size and mass percentage of the SiO₂ nanoparticles were essential parameters affecting the fluidization quality of the composite, accounting for 73.88% and 19.01% of the total contribution, respectively. When the fluidized gas contained alcohols, Ca(OH)₂ coated with hydrophilic silica nanoparticles exhibited high fluidization quality.

Gollsch et al. [43] modified the Ca(OH)₂ powder using nanostructured flow agents (nanostructured silicon and/or aluminum oxide) based on high-intensity dry mixing. By increasing the distance, the adhesion between the particles was reduced, improving the flowability of the powder [44]. The additive improved the fluidity of the powder in the first few cycles. However, after several heat storage cycles, the fluidity of the mixture gradually worsened, whereas that of the pure Ca(OH)₂ powder gradually improved. It was concluded that the nanostructured additive in the mixture reacted with the host particles to form side products, which led to a smooth particle surface and increased the inter-particle forces. However, the inter-particle forces of the pure Ca(OH)₂ powder decreased owing to particle agglomeration. The above-mentioned studies on surface coatings are summarized in Table 3.

Table 3. Summary of research on surface coatings ¹.

Research	Coating	Preparation Method	Benefit
Roßkopf et al. [37,39]	nano-SiO ₂ particles	magnetic agitation	◇ powder agglomeration ↓ ◇ powder flow characteristics ↑ ◇ heat and mass transfer ↑
Xu et al. [40]	nano-SiO ₂ particles	reactive molecular dynamics simulations	◇ powder agglomeration ↓
Amjadi et al. [41,42]	hydrophilic/hydrophobic silica nanoparticles	dry mixing	◇ powder flow characteristics ↑
Gollsch et al. [43]	nanostructured silicon and(or) aluminum oxide	dry mixing	◇ powder flow characteristics ↑

¹ ↑ indicates an increase, and ↓ indicates a decrease.

2.4. Supporting Frames

Kariya et al. [45] selected low-cost vermiculite with high porosity and chemical stability as the Ca(OH)₂ supporting frame and prepared a composite using the impregnation method (Figure 9). The hydration rate of the composite increased with an increasing number of cycles, whereas that of pure Ca(OH)₂ exhibited the opposite trend. The maximum hydration

rate of the composite material ($0.93 \times 10^{-2} \text{ s}^{-1}$) was also higher than that of pure $\text{Ca}(\text{OH})_2$ ($0.71 \times 10^{-2} \text{ s}^{-1}$) at the 15th cycle when the content of $\text{Ca}(\text{OH})_2$ in the composite was 38 wt.%. The authors explained this phenomenon based on reaction kinetics using a grain model, proving that vermiculite can improve cycle stability and solve the problem of a low reaction rate to a certain extent. Kariya and Kato [46] also attempted to use porous silicon carbide with high porosity as the supporting frame for $\text{Ca}(\text{OH})_2$ and found that the maximum hydration rate of the composite material was 1.2 times higher than that of $\text{Ca}(\text{OH})_2$ because the porous support improved the steam diffusion effect.

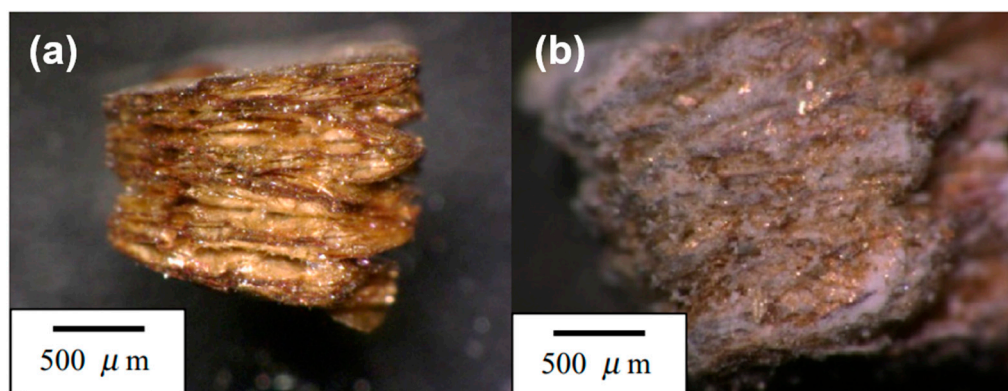


Figure 9. Photos of samples of (a) vermiculite and (b) vermiculite/ $\text{Ca}(\text{OH})_2$ composites. (Reprinted with permission from ref. [45]. Copyright 2015 Elsevier).

Funayama et al. [47,48] used silicon carbide–silicon (SiC–Si) ceramic foam (Figure 10) and a SiC–Si ceramic honeycomb (Figure 11) as the $\text{Ca}(\text{OH})_2$ powder-supporting frame. The ceramic foam composite had a volumetric energy storage density of $440 \text{ kJ L-bed}^{-1}$ and a volumetric heat output rate of $1.3 \text{ kW L-bed}^{-1}$ (for the first 5 min at a maximum hydration pressure of 84.6 kPa). In comparison, the ceramic honeycomb composite had a volumetric energy storage density of $0.76 \text{ MJ L-bed}^{-1}$ and a maximum heat storage power of $0.22 \text{ kW L-bed}^{-1}$; the heat output rate (for the first 5 min at the maximum hydration pressure of 85 kPa) was $1.6 \text{ kW L-bed}^{-1}$. Both supporting frames enhanced the heat transfer of the heat storage materials [49] and prevented the formation of centimeter-scale agglomerates. In a recent study, Funayama et al. [50] used the extrusion method to load a $\text{Ca}(\text{OH})_2$ slurry into a composite foam, further improving the power density and bulk stability of the heat storage material. Both the maximum heat storage power density ($0.36 \text{ MW/m}^3_{\text{bed}}$) and the heat release power density ($0.71 \text{ MW/m}^3_{\text{bed}}$) of the composite foam at 5 min during hydration were 1.6 times that of pure powder. The above-mentioned studies on supporting frames are summarized in Table 4.

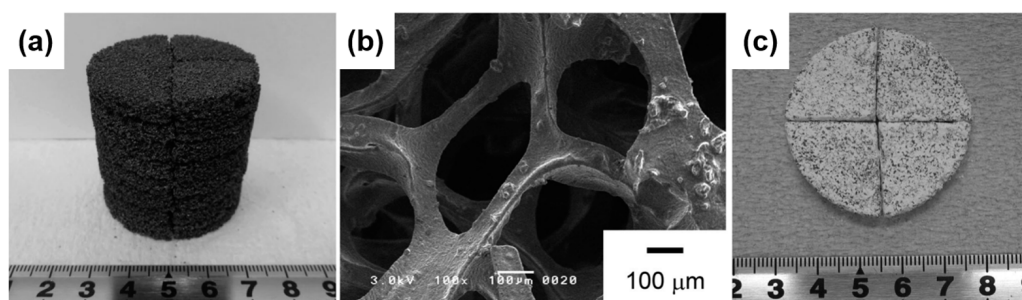


Figure 10. Ceramic foam and composite material: (a) SiC–Si ceramic foam; (b) microstructure of SiC–Si ceramic foam; and (c) SiC–Si ceramic foam/ $\text{Ca}(\text{OH})_2$ composites. (Reprinted with permission from ref. [47]. Copyright 2019 John Wiley & Sons).

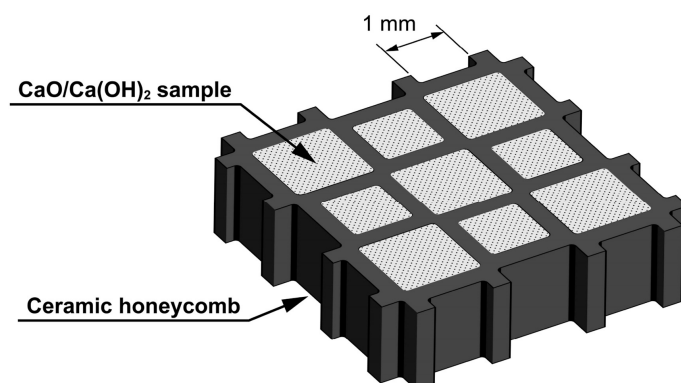


Figure 11. Diagram of SiC-Si ceramic honeycomb/Ca(OH)₂ composite. (Reprinted with permission from ref. [48]. Copyright 2020 Elsevier).

Table 4. Summary of research on supporting frames ¹.

Research	Supporting Frames	Preparation Method	Benefit
Kariya et al. [45]	vermiculite	impregnation	<ul style="list-style-type: none"> ◇ hydration rate ↑ ◇ cycle stability ↑
Kariya and Kato [46]	silicon carbide	impregnation	<ul style="list-style-type: none"> ◇ hydration rate ↑
Funayama et al. [47,48]	SiC-Si ceramic foam/ ceramic honeycomb	vacuum impregnation/compression	<ul style="list-style-type: none"> ◇ heat transfer ↑ ◇ centimeter-scale agglomerates ↓
Funayama et al. [50]	composite foam	extrusion	<ul style="list-style-type: none"> ◇ power density ↑ ◇ bulk stability ↑

¹ ↑ indicates an increase, and ↓ indicates a decrease.

3. Granulated Material Performance Improvement Technology

3.1. Composite Granules

Fujii et al. [51,52] prepared spherical Ca(OH)₂ pellets (diameter of ~17 mm) and cylindrical Ca(OH)₂ pellets (diameter = 19.5 mm; length = 60 mm). The specific volume of Ca(OH)₂ (0.45 cm³/g) was larger than that of CaO (0.29 cm³/g). During heat storage, Ca(OH)₂ decomposition led to a contraction in the geometric size of the pellets, and the volume of the pellets expanded during the heat release process. This alternating shrinkage and expansion caused cracking. Adding 15 wt.% Al was also found to enhance dehydration while maintaining the geometric shape. Based on the XRD patterns, Ca₃Al₂(OH)₁₂ and Ca₁₂Al₁₄O₃₃ were identified as the main factors enhancing the brittleness of the pellets.

Funayama et al. [53] used a packed bed reactor with a 100 W scale to evaluate 60 g of cylindrical Ca(OH)₂ pellets (diameter = 1.9 mm; length = 2–10 mm). The experimental results showed that the heat storage density of the bed was 1.0 MJ L-bed⁻¹, and the average heat output power in the first 10 min was 0.71 kW L-bed⁻¹ with an initial bed temperature of 350 °C and a hydration pressure of 84.6 kPa. The Ca(OH)₂ pellets maintained a stable conversion over 17 cycles.

Gupta et al. [54] added the inert additive calcium titanate (CaTiO₃) to Ca(OH)₂ composite pellets (diameter = 3.2 mm; length = 5.6 mm) to improve the reaction rate and structural stability. Inert CaTiO₃ particles acted as skeletal supports in the Ca(OH)₂ pellets, which greatly reduced the influence of the conversion between Ca(OH)₂ and CaO on the pellet volume and improved the integrity of the overall pellet structure. The CaTiO₃ skeleton was conducive to steam diffusion while maintaining the pellet structure, and provided a larger reaction area and improved reaction rate. When the mass ratio of Ca(OH)₂ to CaTiO₃ in the composite pellets was 1:0.5 or 1:1, the mechanical strength of the composite

pellets was more than 50% higher than that of pure $\text{Ca}(\text{OH})_2$ pellets. The above-mentioned studies on composite granules are summarized in Table 5.

Table 5. Summary of research on composite granules ¹.

Research	Granule Shape	Additives	Benefit
Fujii et al. [51,52]	spherical/cylindrical pellets	Al	◇ dehydration rate ↑ ◇ maintaining the geometric shape
Funayama et al. [53]	cylindrical pellets	none	◇ maintain a stable conversion
Gupta et al. [54]	cylindrical pellets	CaTiO_3	◇ dehydration rate ↑ ◇ structural stability ↑

¹ ↑ indicates an increase, and ↓ indicates a decrease.

3.2. Surface Coatings

Valverde-Pizarro et al. [55] coated composite pellets (60 wt.% $\text{Ca}(\text{OH})_2$ and 40 wt.% $\gamma\text{-Al}_2\text{O}_3$) with mesoporous alumina by dip coating and added cetyltrimethylammonium bromide surfactant during the coating process. After 10 cycles, the hydration conversion of the composite was >80%, and the heat release was >800 kJ/kg. After 20 cycles, the composite retained a spherical structure, and there were highly dispersed alumina particles on its surface, but cracks also appeared (Figure 12). The authors suggested that the surfactants not only reduced the surface tension of the pellets and slowed the generation of cracks, but also made the coating more uniform, and increased the compressive strength. Cosquillo Mejia et al. [56] performed 10 heat storage cycles using this material in a moving bed reactor. The results confirmed that alumina coating can improve the mechanical stability of composite pellets under reaction conditions.

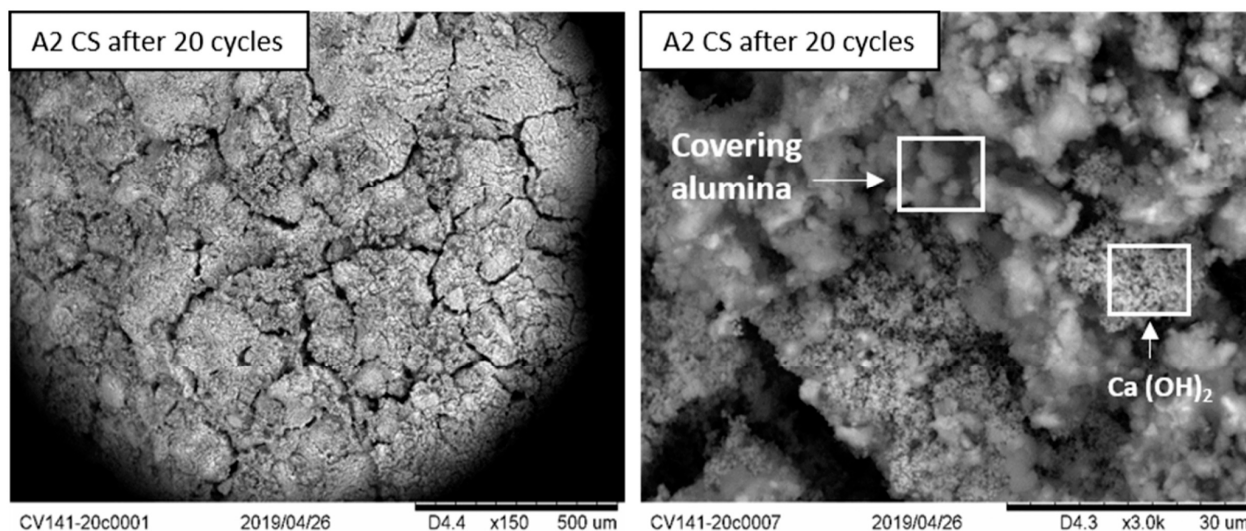


Figure 12. Microscopic images of mesoporous alumina-coated composite pellets after 20 heat storage cycles. (Reprinted with permission from ref. [55]. Copyright 2020 Elsevier).

Briones et al. [57] coated dense silica and Al-mesoporous silica gel onto the surface of spherical and cylindrical composite pellets (60 wt.% $\text{Ca}(\text{OH})_2$ and 40 wt.% $\gamma\text{-Al}_2\text{O}_3$), respectively, using a dip coating method. When calcined, both gels form a hard calcium silicate layer, helping to maintain the structural integrity of the sample during the cycle. The former forms a continuous coating on the surface of the composite pellet, providing a high-intensity value (up to 31 N) for the pellet. The latter forms a porous silica coating on the surface of the composite pellet, which helps maintain the porosity of the pellet, thus promoting steam diffusion. After 10 cycles, the cylindrical samples showed higher

hardness values and hydration yields than the spherical samples. The above-mentioned studies on granule surface coatings are summarized in Table 6.

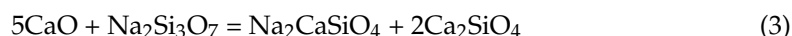
Table 6. Summary of research on granule surface coatings ¹.

Research	Granule Shape	Coating	Benefit
Valverde-Pizarro et al. [55]	spherical pellets	mesoporous alumina	<ul style="list-style-type: none"> ◇ cycle stability ↑ ◇ structural stability ↑
Cosquillo Mejia et al. [56]	spherical pellets	mesoporous alumina	<ul style="list-style-type: none"> ◇ structural stability ↑ ◇ maintain the structural integrity ◇ dense silica gel providing a high-intensity value
Briones et al. [57]	spherical/cylindrical pellets	dense silica gel/Al-mesoporous silica gel	<ul style="list-style-type: none"> ◇ Al-mesoporous silica gel helps to maintain the porosity ◇ cylindrical pellets showed higher hardness values and hydration yields

¹ ↑ indicates an increase, and ↓ indicates a decrease.

3.3. Binder Matrices

Criado et al. [58] prepared cylindrical composite pellets (length = 1–3 mm; diameter = 2 mm) using limestone as the precursor for CaO and sodium silicate as the binder. In the process of obtaining composite materials rich in CaO via calcination at 850 °C, CaO reacts with sodium silicate (Equation (3)) to produce hard Ca silicates. This yielded a composite material with a compressive strength approximately four times that of the original CaO. However, the CaO content of the composite material was reduced. The authors suggested that the most suitable CaCO₃ parameters were a particle size of 36–63 μm for the Ca precursor, a Ca/Si molar ratio of 4.8–6.2, and calcination performed in air at 850 °C. After 500 hydration (450 °C pure steam)/dehydration (500 °C air) cycles, the composite maintained a stable conversion. However, when the heat storage atmosphere was pure steam, the hydration conversion of the composite decreased sharply with the number of cycles. XRD analysis showed that hydrated silicates were generated when dehydrated in a steam atmosphere, which hindered the hydration of CaO and led to the attenuation of the hydration conversion (Figure 13). Criado et al. [59] reported that in the process of converting CaO into Ca(OH)₂, a larger grain size causes the fracture of the hard Ca silicate framework and reduces the compressive strength. They also pointed out that the mechanical strength of the composite materials can be maintained by providing CaO particles with a larger space. In one method, CaCO₃ was used as a CaO precursor to provide space for Ca(OH)₂ grain growth based on the difference in molar volume (36.9 cm³/mol for CaCO₃ and 16.9 cm³/mol for CaO). In another method, the hydration conversion of CaO was controlled to improve the mechanical stability of the pellets.



Sakellariou et al. [60] used calcium nitrate and calcium acetate as CaO precursors, and CaO/Al₂O₃ composites were obtained using liquid-phase self-propagating high-temperature synthesis. A polyvinyl alcohol aqueous solution was used as a binder to prepare the pellets (diameter = 30 mm; length = 5 mm). The experimental results showed that the composite with calcium nitrate as the CaO precursor exhibited a better hydration/dehydration performance. The presence of Al resulted in more Ca₃Al₂O₆ and Ca₁₂Al₁₄O₃₃ in the composite. A mixed Ca/Al phase does not participate in the heat

storage and release process but can dampen the effects of cyclic dehydration–hydration (shrinking–swelling mechanism) and enhance pellet structural integrity. Based on their observations, the authors reported that Ca/Al composites with calcium nitrate as a precursor, close to 81/19, possess a high heat storage capacity and mechanical strength. To reduce material costs, Sakellariou et al. [61,62] selected natural limestone as the CaO precursor and developed near-spherical (850 μm –2 mm diameter) composites using 25 wt.% kaolinite ($\text{Al}_2(\text{Si}_2\text{O}_5)(\text{OH})_4$) as the binder. After 20 cycles, the composites remained intact and exhibited a high mechanical strength. The XRD analysis showed that the $\text{Ca}_2\text{Al}_2\text{SiO}_7$ formed in the composite pellets had a higher mechanical strength. The microscopic image shows that the CaO particles in the composite pellets were wrapped in a smooth and compact $\text{Ca}_2\text{Al}_2\text{SiO}_7$ network structure (Figure 14). While this improved the compressive strength of the composite pellets, it also consumed some CaO and reduced the heat storage capacity.

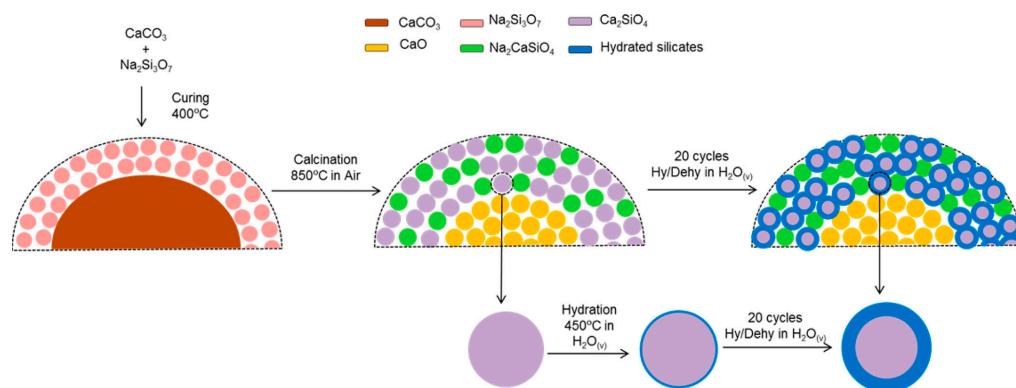


Figure 13. Mechanism of CaO hydration performance degradation caused by dehydration in pure steam. (Reprinted with permission from ref. [58]. Copyright 2015 American Chemical Society).

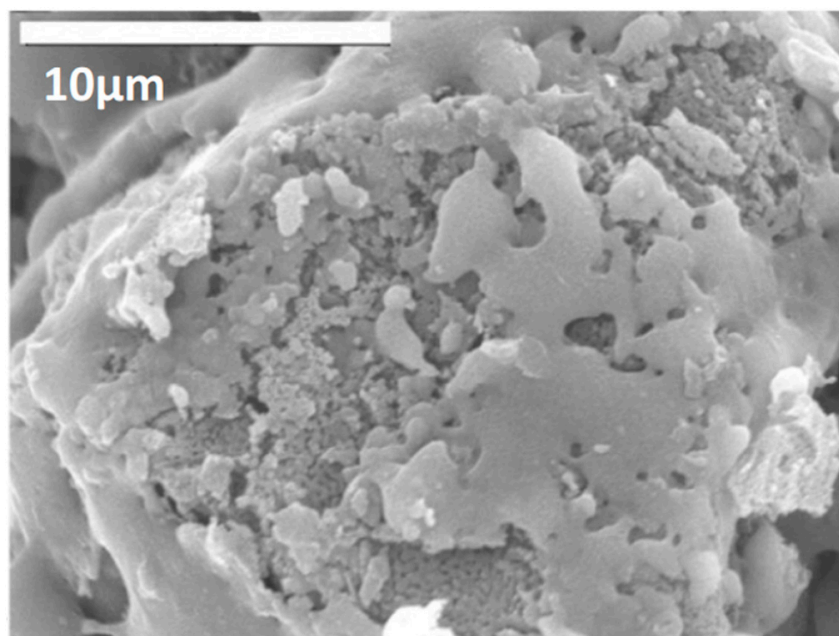


Figure 14. Microscopic images of kaolinite/CaO composite. (Reprinted with permission from ref. [62]. Copyright 2017 Elsevier).

Xia et al. [63] prepared a tablet-shaped composite (diameter = 8 mm; height = 6 mm) via ball milling using carboxymethyl cellulose sodium (CMC-Na) as the binder and vermiculite as the raw material. Compared with powdery $\text{Ca}(\text{OH})_2$, when the composite ratio (CaO: CMC-Na: vermiculite) was 80:15:5, the gravimetric storage density of the composite material was 71% of that of the pure material, and the volumetric storage density was 124% of that of

the pure material. The CMC-Na in the composite formed mesh structures under the influence of carbonization and sintering. The mesh structure and vermiculite skeleton provided structural support for the composite material and separated the heat storage material particles, thereby reducing agglomeration. The above-mentioned studies on granule binder matrices are summarized in Table 7.

Table 7. Summary of research on granule binder matrices ¹.

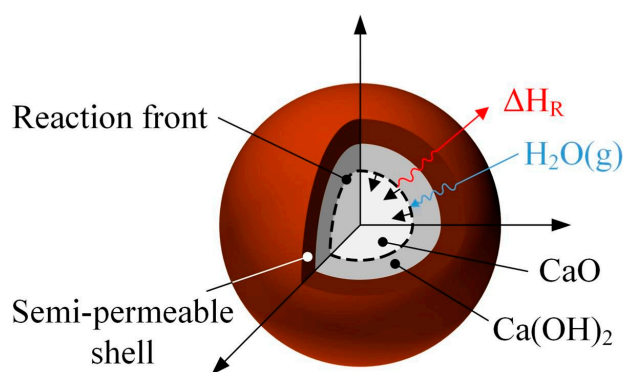
Research	Granule Shape	Binder Matrices	Benefit
Criado et al. [58,59]	cylindrical pellets	sodium silicate	<ul style="list-style-type: none"> ◇ structural stability ↑ ◇ maintain a stable conversion
Sakellariou et al. [60]	cylindrical pellets	polyvinyl alcohol	<ul style="list-style-type: none"> ◇ hydration/dehydration performance ↑ ◇ structural stability ↑
Sakellariou et al. [61,62]	near-spherical pellets	kaolinite	<ul style="list-style-type: none"> ◇ structural stability ↑
Xia et al. [63]	cylindrical pellets	CMC-Na	<ul style="list-style-type: none"> ◇ volumetric storage density ↑ ◇ structural stability ↑

¹ ↑ indicates an increase, and ↓ indicates a decrease.

3.4. Macro-Encapsulation

Afflerbach et al. [64] proposed an oxide ceramic-based material for the semipermeable encapsulation of pre-granulated $\text{Ca}(\text{OH})_2$ based on the core-shell principle. The basic principles of mass and heat transfer in heat storage and release processes are shown in Figure 15 [65]. The actual setup is shown in Figure 16, where the white ball core is the heat storage material and the red shell is the oxide ceramic material. Ceramic materials exhibit high thermal stability and mechanical strength after sintering at high temperatures; however, a small amount of larnite by-products can be produced. The decomposition and release of organic compounds during ceramic sintering can form a porous network structure in the ceramic shell, which is conducive to steam diffusion. A ratio of $\text{Ca}(\text{OH})_2$ /adhesion-promoting agent/dry ceramic precursor powder of 4:2:3 may be the best choice. The heat storage material in the ceramic shell was completely transformed in 10 cycles, and its compressive strength showed little change, decreasing from 86.7 N to 82.6 N. The gravimetric storage density of the encapsulation material was 56–58%, and the volumetric storage density was 33% that of pure CaO , which was determined by the mass proportion of the ceramic shell in the encapsulation material.

Hydration reaction
(Discharging)



Dehydration reaction
(Charging)

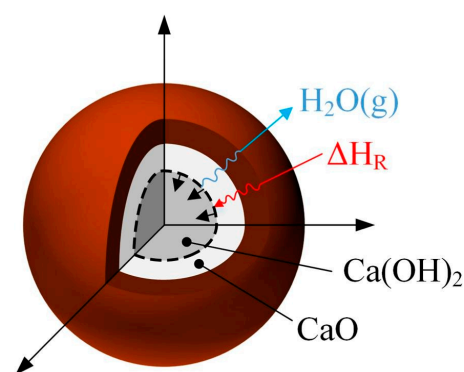


Figure 15. Schematic diagram of heat and H_2O transfer of semi-permeable encapsulation materials during heat storage and release. (Reprinted with permission from ref. [65]. Copyright 2021 Elsevier).

Gollsch et al. [66] verified the mechanical stability of an encapsulation material in a laboratory-scale reactor. Furthermore, Afflerbach et al. [65] increased the compressive strength of these materials by approximately 15% by adding 5 wt.% diatomaceous earth to the powdery ceramic precursor. This increased the amorphous glass phase in the ceramic shell and promoted densification of the shell microstructure, which not only improved the mechanical strength but also significantly enhanced the bulk thermal conductivity of the material. Compared with the unencapsulated materials, the thermal conductivity of the encapsulated materials was improved by up to 60%. The energy storage density of the encapsulated material was 144.9 kWh/m³ and 0.16 kWh/kg.

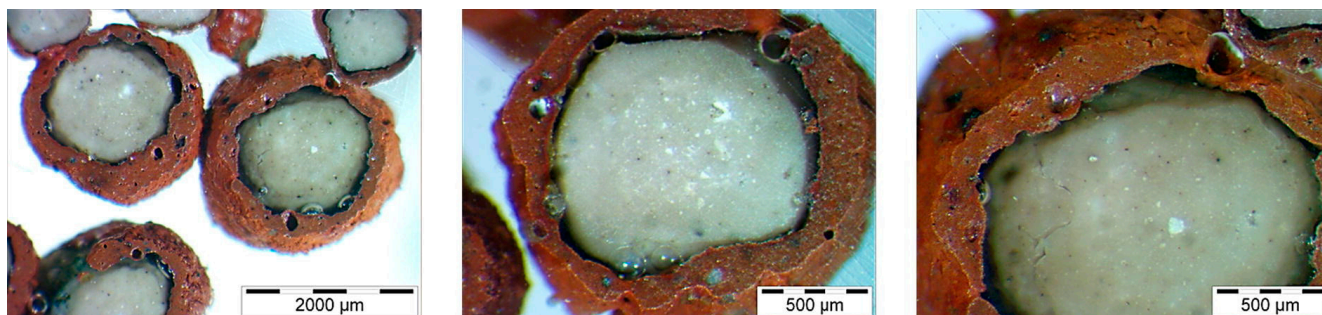


Figure 16. Sectional photo of oxide ceramic-based semi-permeable encapsulation material. (Reprinted with permission from ref. [64]. Copyright 2017 Elsevier).

Cosquillo Mejia et al. [67] conducted studies on the heat storage of ceramic-encapsulated materials in an indirect heat transfer moving bed reactor and found that ceramic-encapsulated materials had good fluidity and did not plug heat exchangers; however, the shells of some ceramic-encapsulated materials were cracked and broken. At the same time, the heat storage material was not fully transformed under the reactor operating conditions, which was attributed to the mass transfer resistance caused by the ceramic shell in a lower-steam-pressure atmosphere. Guo et al. [68] embedded a mixture of CaCO₃ and carboxymethyl cellulose in a silicon carbide honeycomb matrix and obtained composite pellets via calcination. The composite pellets exhibited good structural stability over 22 cycles, with a discharging/charging density of over 1000 kJ/L_{pellet}. The above-mentioned studies on granule macro-encapsulation are summarized in Table 8.

Table 8. Summary of research on granule macro-encapsulation ¹.

Research	Encapsulation Materials	Benefit
Afflerbach et al. [64]	oxide ceramic-based material	<ul style="list-style-type: none"> ◇ thermal stability ↑ ◇ structural stability ↑ ◇ porous shell
Gollsch et al. [66]	oxide ceramic-based material	<ul style="list-style-type: none"> ◇ maintain structural stability in a laboratory-scale fixed-bed reactor
Afflerbach et al. [65]	oxide ceramic-based material and diatomaceous earth	<ul style="list-style-type: none"> ◇ structural stability ↑ significantly ◇ bulk thermal conductivity ↑
Cosquillo Mejia et al. [67]	oxide ceramic-based material and diatomaceous earth and Na ₂ CO ₃	<ul style="list-style-type: none"> ◇ good fluidity in an indirect heat-transfer moving bed reactor
Guo et al. [68]	silicon carbide	<ul style="list-style-type: none"> ◇ structural stability ↑

¹ ↑ indicates an increase, and ↓ indicates a decrease.

4. Problems and Suggestions

Based on the reviewed literature, each technology can improve various properties of $\text{Ca}(\text{OH})_2$ while also creating other problems, and, currently, no single technology can solve all of these problems. A reasonable approach is to select the most appropriate technology according to the practical application of the strengthening demand for specific aspects of heat storage materials or to combine various technologies. Bayon et al. [69] found that feedstock cost accounts for a major part of the capital cost after an economic evaluation of 17 thermochemical energy storage systems based on gas–solid reaction. For a composite material based on $\text{Ca}(\text{OH})_2$, the material cost mainly comprises additive and processing costs. With an increase in the cycle number and carbonation of heat storage materials under the influence of CO_2 in the air, performance gradually declines, and fresh materials are needed [70]. Therefore, to achieve large-scale industrial applications, it is necessary to screen cheaper additives and use a relatively simple preparation process so that the material costs remain acceptable. At the same time, reactions between the added functional material and heat storage material should be avoided as much as possible, as this significantly reduces the content of the effective heat storage material. These are common issues that all technologies must address. The individual problems and suggestions related to specific technologies for future development are summarized as follows:

- Small amounts of elements can be doped to change the properties of heat storage materials. A small amount of doping material has little effect on the heat storage capacity of the material and can significantly improve its kinetic characteristics. Earlier studies mainly focused on the doping effect of a single element, whereas more recent studies have focused on the co-doping effect based on relatively inexpensive elements. Simultaneously, more attention should be paid to the mechanisms of doping modifications;
- The main purpose of constructing composite materials (powders or granules) is to introduce other substances with excellent properties into $\text{Ca}(\text{OH})_2$ to compensate for the shortage of heat storage materials, such as high-thermal-conductivity materials that improve the heat transfer effect. Because the heat storage capacity of a composite material includes the thermochemical heat storage capacity of $\text{Ca}(\text{OH})_2/\text{CaO}$ and the sensible heat storage capacity of all substances, the excessive addition of functional materials reduces the heat storage capacity of the composite. Therefore, it is necessary to explore advanced functional materials to reduce the amount of added material while maintaining the performance of the composite materials;
- Coating nanoparticles onto the surface of a powder or granulated material can reduce adhesion forces and stabilize the surface structure of the material. Because the volume and surface structure of the host particles change during heat storage cycles, a higher coverage quality is required to enable the nanoparticles to adapt to changes in the host particles;
- The supporting frames and binder matrices can improve the structural integrity of heat storage materials. These materials occupy a high proportion of the composite material, which significantly reduces the energy storage density of the composite. For supporting frame technology, skeleton materials with high porosity should be developed to improve the loading capacity of heat storage materials. For binder matrix technology, the particle structure should be maintained, whereas the amount of binder added should be reduced to improve the energy storage density;
- Macro-encapsulation provides excellent mechanical strength and can maintain the structure of heat storage materials for a long time. As inert shell materials occupy a certain space and exhibit mass transfer resistance, it is necessary to ensure acceptable compressive strength while reducing shell thickness and improving permeability to improve heat storage rates and capacities.

In addition to these performance-improving technologies, advanced technologies in other fields should also be used as references. For example, Huang et al. [71] regulated the crystal morphology of $\text{Ca}(\text{OH})_2$ at the microscopic level and showed that $\text{Ca}(\text{OH})_2$ nanoparticles with a spindle structure (Figure 17a) were superior to those with a hexagonal structure. Bian et al. [72] prepared hollow nanostructured CaO (HN- CaO) using glucose as

the carbon template (Figure 17b) and reported that its hollow structure has the advantages of high porosity, large surface area, and high gas diffusion efficiency [73]. Therefore, the diffusion resistance of steam is significantly reduced, and a high conversion rate is achieved. Newly developed heat storage materials should also be tested in larger-scale reactors to evaluate their ability to withstand mechanical and thermal stresses on a bulk scale.

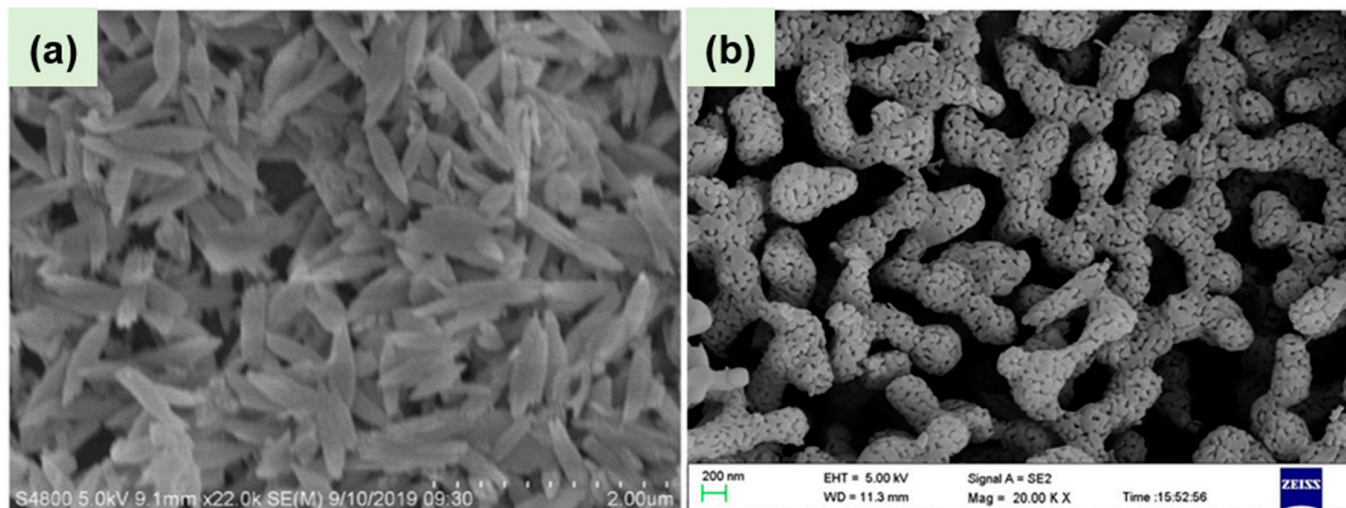


Figure 17. Microscopic images of (a) spindle-shaped $\text{Ca}(\text{OH})_2$ nanomaterials and (b) HN-CaO. (Reprinted with permission from ref. [71]. Copyright 2019 Springer Nature) (Reprinted with permission from ref. [72]. Copyright 2021 Elsevier).

5. Carbide Slag Can Replace High-Quality $\text{Ca}(\text{OH})_2$ for Heat Storage

Carbide slag is a by-product of the calcium carbide method used to produce polyvinyl chloride (PVC), the main component of which is $\text{Ca}(\text{OH})_2$. The annual output of carbide slag in China, as a bulk industrial solid waste, is almost 34 million tons. In 2018, Yuan et al. [74] proposed the use of carbide slag instead of high-quality $\text{Ca}(\text{OH})_2$ for heat storage and demonstrated its potential for long-term thermochemical heat storage over 30 heat storage cycles. Zhang et al. [75] modified carbide slag with a by-product of biodiesel (more than 90% glycerol), obtained a porous and loose structure, and reduced the diffusion resistance of steam. After 30 cycles, the hydration conversion and heat storage density of the modified carbide slag were 0.65 mol/mol and 1.14 GJ/t, respectively, which was 1.6 times that of the original carbide slag. Subsequently, Zhang et al. [76] prepared Ca/Mg-based composites using carbide slag with dolomite ($\text{CaMg}(\text{CO}_3)_2$) as the raw material and found that a small amount of MgO maintained good pore characteristics, whereas excessive MgO hindered steam diffusion. Feng et al. [77–79] also systematically studied the thermodynamic characteristics (including thermal stability, heat storage capacity, and heat transfer characteristics) and reaction kinetics of carbide slag (Figure 18). They showed that while the thermochemical heat storage capacity of carbide slag was lower than that of pure $\text{Ca}(\text{OH})_2$, its sensible heat storage capacity was higher than that of pure $\text{Ca}(\text{OH})_2$. Under the same conditions, the reaction rate of the carbide slag was almost the same as that of pure $\text{Ca}(\text{OH})_2$; however, the heat storage rate was lower because of differences in purity. Considering that carbide slag is an industrial solid waste, its near-zero material cost and good heat storage performance indicate its high potential for large-scale thermochemical heat storage applications.

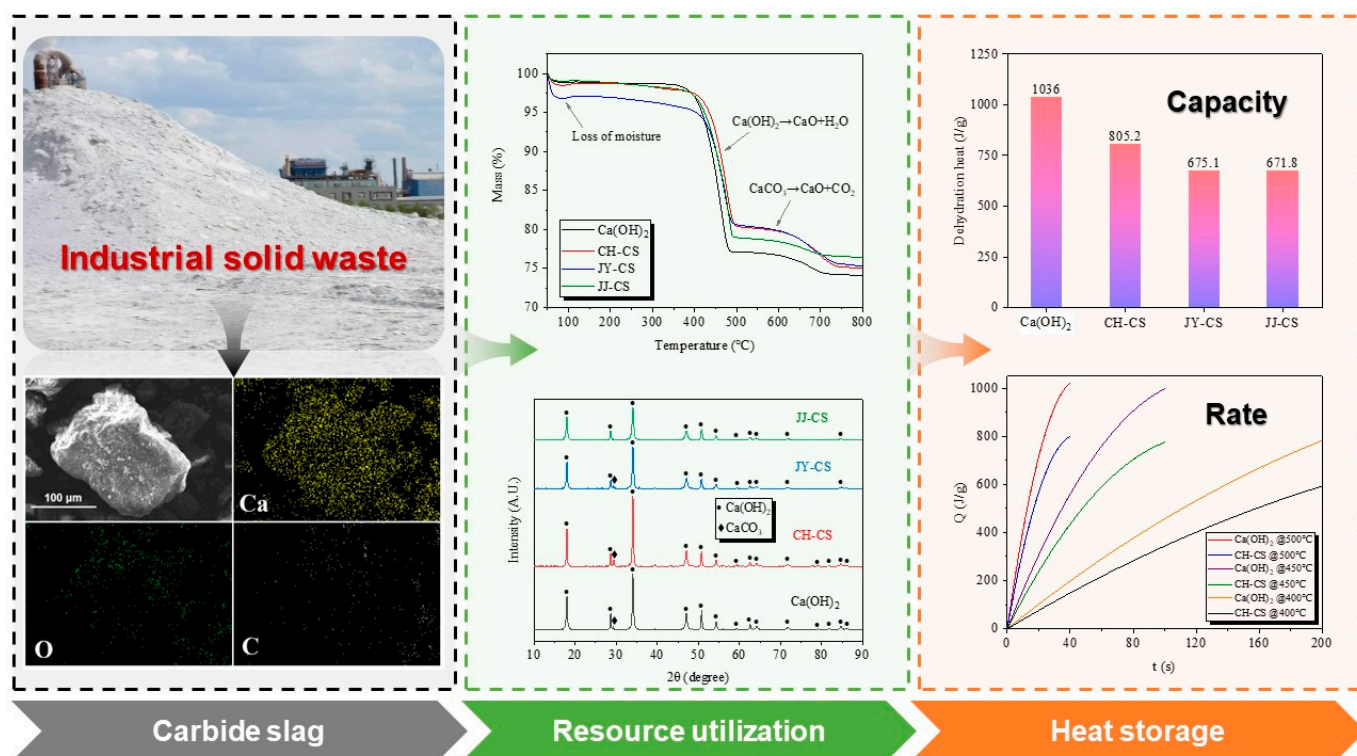


Figure 18. Thermodynamic and kinetic characteristics of carbide slag for heat storage. (Reprinted with permission from ref. [79]. Copyright 2022 Elsevier.).

6. Conclusions

Heat storage and release through the reversible reaction of $\text{Ca}(\text{OH})_2$ dehydration and CaO hydration is a thermochemical energy storage scheme with potential industrial applications. This study reviewed opportunities for improving the performance of $\text{Ca}(\text{OH})_2/\text{CaO}$ heat storage materials, existing problems, and opportunities for future development. The main conclusions are as follows:

- Heat storage materials can be divided into powders and granulated materials based on their macroscopic morphologies. Performance improvement technologies for powder materials include doping modifications, composite powders, surface coatings, and supporting frames. Technologies for improving the performance of granulated materials include composite granules, surface coatings, binder matrices, and macro-encapsulation. Currently, no technology can simultaneously improve the energy storage density, energy storage rate, and cycling stability of heat storage materials. Therefore, relevant technologies should be selected according to the main characteristics that must be improved for specific practical applications;
- The functional materials used in existing research can regulate heat storage characteristics by changing the crystal structure of $\text{Ca}(\text{OH})_2/\text{CaO}$ and can also compensate for the deficiencies of $\text{Ca}(\text{OH})_2/\text{CaO}$ owing to several advantages. The addition of functional materials is usually accompanied by a relevant preparation process, thus increasing the cost of the heat storage materials. At present, the competitiveness of heat storage materials can be improved by reducing material and manufacturing costs. Strategies to reduce material costs include using inexpensive functional materials and choosing carbide slag to replace high-quality $\text{Ca}(\text{OH})_2$. Reducing manufacturing costs can involve choosing simpler and more effective manufacturing technologies;
- Improvements in heat storage performance include heat storage capacity, thermal conductivity, reaction rate, and structural stability. The improvement in heat storage performance is inevitably accompanied by a reduction in heat storage capacity, which is caused by the addition of other materials. The structural stability of heat storage

materials affects the heat and mass transfer effects as well as the reaction rate. Increasing the porosity of a material reduces its mechanical strength but achieves a high reaction rate. Thus, the heat storage properties and structural stability of the materials are interrelated.

Author Contributions: Conceptualization, Y.F. and X.L.; methodology, Y.F.; investigation, Y.F., H.W. and C.L.; writing—original draft preparation, Y.F.; writing—review and editing, X.L. and H.Y.; supervision, M.Z.; project administration, H.Y. All authors have read and agreed to the published version of the manuscript.

Funding: This research was funded by State Key Laboratory of Power System and Generation Equipment (SKLD21M13).

Data Availability Statement: The data presented in this study are available in this article.

Conflicts of Interest: The authors declare no conflict of interest.

References

1. Net Zero by 2050—A Roadmap for the Global Energy Sector. Available online: <https://www.iea.org/reports/net-zero-by-2050> (accessed on 26 January 2023).
2. Steffen, B.; Weber, C. Efficient storage capacity in power systems with thermal and renewable generation. *Energy Econ.* **2013**, *36*, 556–567. [[CrossRef](#)]
3. Hirth, L.; Ziegenhagen, I. Balancing power and variable renewables: Three links. *Renew. Sustain. Energy Rev.* **2015**, *50*, 1035–1051. [[CrossRef](#)]
4. Tian, Y.; Zhao, C. A review of solar collectors and thermal energy storage in solar thermal applications. *Appl. Energy* **2013**, *104*, 538–553. [[CrossRef](#)]
5. Thess, A. Thermodynamic efficiency of pumped heat electricity storage. *Phys. Rev. Lett.* **2013**, *111*, 110602. [[CrossRef](#)] [[PubMed](#)]
6. Okazaki, T.; Shirai, Y.; Nakamura, T. Concept study of wind power utilizing direct thermal energy conversion and thermal energy storage. *Renew. Energy* **2015**, *83*, 332–338. [[CrossRef](#)]
7. Chen, H.; Cong, T.; Yang, W.; Tan, C.; Li, Y.; Ding, Y. Progress in electrical energy storage system: A critical review. *Prog. Nat. Sci.* **2009**, *19*, 291–312. [[CrossRef](#)]
8. Zhang, H.; Baeyens, J.; Cáceres, G.; Degrève, J.; Lv, Y. Thermal energy storage: Recent developments and practical aspects. *Prog. Energy Combust. Sci.* **2016**, *53*, 1–40. [[CrossRef](#)]
9. Pelay, U.; Luo, L.; Fan, Y.; Stitou, D.; Rood, M. Thermal energy storage systems for concentrated solar power plants. *Renew. Sustain. Energy Rev.* **2017**, *79*, 82–100. [[CrossRef](#)]
10. Alva, G.; Lin, Y.; Fang, G. An overview of thermal energy storage systems. *Energy* **2018**, *144*, 341–378. [[CrossRef](#)]
11. Miró, L.; Gasia, J.; Cabeza, L. Thermal energy storage (TES) for industrial waste heat (IWH) recovery: A review. *Appl. Energy* **2016**, *179*, 284–301. [[CrossRef](#)]
12. Kuravi, S.; Trahan, J.; Goswami, D.; Rahman, M.; Stefanakos, E. Thermal energy storage technologies and systems for concentrating solar power plants. *Prog. Energy Combust. Sci.* **2013**, *39*, 285–319. [[CrossRef](#)]
13. Wentworth, W.; Chen, E. Simple thermal decomposition reactions for storage of solar thermal energy. *Sol. Energy* **1976**, *18*, 205–214. [[CrossRef](#)]
14. Gil, A.; Medrano, M.; Martorell, I.; La 'zaro, A.; Dolado, P.; Zalba, B.; Cabeza, L. State of the art on high temperature thermal energy storage for power generation. Part 1-Concepts, materials and modellization. *Renew. Sustain. Energy Rev.* **2010**, *14*, 31–55. [[CrossRef](#)]
15. André, L.; Abanades, S.; Flamant, G. Screening of thermochemical systems based on solid-gas reversible reactions for high temperature solar thermal energy storage. *Renew. Sustain. Energy Rev.* **2016**, *64*, 703–715. [[CrossRef](#)]
16. Pardo, P.; Deydier, A.; Anxionnaz-Minvielle, Z.; Rougé, S.; Cabassud, M.; Cognet, P. A review on high temperature thermochemical heat energy storage. *Renew. Sustain. Energy Rev.* **2014**, *32*, 591–610. [[CrossRef](#)]
17. Solé, A.; Fontanet, X.; Barreneche, C.; Fernández, A.; Martorell, I.; Cabeza, L. Requirements to consider when choosing a thermochemical material for solar energy storage. *Sol. Energy* **2013**, *97*, 398–404. [[CrossRef](#)]
18. Schaube, F.; Wörner, A.; Tamme, R. High temperature thermochemical heat storage for concentrated solar power using gas–solid reactions. *J. Sol. Energy Eng.* **2011**, *133*, 031006. [[CrossRef](#)]
19. Carrillo, A.; Gonzalez-Aguilar, J.; Romero, M.; Coronado, J. Solar energy on demand: A review on high temperature thermochemical heat storage systems and materials. *Chem. Rev.* **2019**, *119*, 4777–4816. [[CrossRef](#)]
20. Criado, Y.; Alonso, M.; Abanades, J. Kinetics of the CaO/Ca(OH)₂ hydration/dehydration reaction for thermochemical energy storage applications. *Ind. Eng. Chem. Res.* **2014**, *53*, 12594–12601. [[CrossRef](#)]
21. Yan, J.; Zhao, C. Experimental study of CaO/Ca(OH)₂ in a fixed-bed reactor for thermochemical heat storage. *Appl. Energy* **2016**, *175*, 277–284. [[CrossRef](#)]

22. Guo, R.; Funayama, S.; Kim, S.; Harada, T.; Takasu, H.; Kato, Y. Hydration reactivity enhancement of calcium oxide-based media for thermochemical energy storage. *Energy Storage* **2021**, *3*, e232. [[CrossRef](#)]
23. Shkatulov, A.; Aristov, Y. Calcium hydroxide doped by KNO_3 as a promising candidate for thermochemical storage of solar heat. *RSC Adv.* **2017**, *7*, 42929–42939. [[CrossRef](#)]
24. Yuan, Y.; Li, Y.; Zhao, J. Development on thermochemical energy storage based on CaO-based materials: A review. *Sustainability* **2018**, *10*, 2660. [[CrossRef](#)]
25. Wang, K.; Yan, T.; Li, R.; Pan, W. A review for $\text{Ca(OH)}_2/\text{CaO}$ thermochemical energy storage systems. *J. Energy Storage* **2022**, *50*, 104612. [[CrossRef](#)]
26. Murthy, M.; Raghavendrachar, P.; Sriram, S. Thermal decomposition of doped calcium hydroxide for chemical energy storage. *Sol. Energy* **1986**, *36*, 53–62. [[CrossRef](#)]
27. Yan, J.; Zhao, C. First-principle study of $\text{CaO}/\text{Ca(OH)}_2$ thermochemical energy storage system by Li or Mg cation doping. *Chem. Eng. Sci.* **2014**, *117*, 293–300. [[CrossRef](#)]
28. Yan, J.; Zhao, C. Thermodynamic and kinetic study of the dehydration process of $\text{CaO}/\text{Ca(OH)}_2$ thermochemical heat storage system with Li doping. *Chem. Eng. Sci.* **2015**, *138*, 86–92. [[CrossRef](#)]
29. Shkatulov, A.; Aristov, Y. Modification of magnesium and calcium hydroxides with salts: An efficient way to advanced materials for storage of middle-temperature heat. *Energy* **2015**, *85*, 667–676. [[CrossRef](#)]
30. Wang, T.; Zhao, C.; Yan, J. Investigation on the $\text{Ca(OH)}_2/\text{CaO}$ thermochemical energy storage system with potassium nitrate addition. *Sol. Energy Mater. Sol. Cells* **2020**, *215*, 110646. [[CrossRef](#)]
31. Maruyama, A.; Kurosawa, R.; Ryu, J. Effect of lithium compound addition on the dehydration and hydration of calcium hydroxide as a chemical heat storage material. *ACS Omega* **2020**, *5*, 9820–9829. [[CrossRef](#)]
32. Bian, Z.; Li, Y.; Wang, F.; Fang, Y.; Zhao, J.; Qi, J. Understanding the acceleration effect of manganese and cerium doping on the hydration of CaO in $\text{CaO}/\text{Ca(OH)}_2$ heat storage by density function theory. *J. Energy Storage* **2022**, *56*, 105953. [[CrossRef](#)]
33. Kariya, J.; Ryu, J.; Kato, Y. Reaction performance of calcium hydroxide and expanded graphite composites for chemical heat storage applications. *ISIJ Int.* **2015**, *55*, 457–463. [[CrossRef](#)]
34. Huang, C.; Xu, M.; Huai, X. Experimental investigation on thermodynamic and kinetic of calcium hydroxide dehydration with hexagonal boron nitride doping for thermochemical energy storage. *Chem. Eng. Sci.* **2019**, *206*, 518–526. [[CrossRef](#)]
35. Li, Y.; Li, M.; Xu, Z.; Meng, Z.; Wu, Q. Dehydration kinetics and thermodynamics of $\text{ZrO}(\text{NO}_3)_2$ -doped Ca(OH)_2 for chemical heat storage. *Chem. Eng. J.* **2020**, *399*, 125841. [[CrossRef](#)]
36. Sun, C.; Yan, X.; Li, Y.; Zhao, J.; Wang, Z.; Wang, T. Coupled CO_2 capture and thermochemical heat storage of CaO derived from calcium acetate. *Greenh. Gases Sci. Technol.* **2020**, *10*, 1027–1038. [[CrossRef](#)]
37. Roßkopf, C.; Haas, M.; Faik, A.; Linder, M.; Wörner, A. Improving powder bed properties for thermochemical storage by adding nanoparticles. *Energy Convers. Manag.* **2014**, *86*, 93–98. [[CrossRef](#)]
38. Kojima, T.; Elliott, J. Effect of silica nanoparticles on the bulk flow properties of fine cohesive powders. *Chem. Eng. Sci.* **2013**, *101*, 315–328. [[CrossRef](#)]
39. Roßkopf, C.; Afflerbach, S.; Schmidt, M.; Görtz, B.; Kowald, T.; Linder, M.; Trettin, R. Investigations of nano coated calcium hydroxide cycled in a thermochemical heat storage. *Energy Convers. Manag.* **2015**, *97*, 94–102. [[CrossRef](#)]
40. Xu, M.; Huai, X.; Cai, J. Agglomeration behavior of calcium hydroxide/calcium oxide as thermochemical heat storage material: A reactive molecular dynamics study. *J. Phys. Chem. C* **2017**, *121*, 3025–3033. [[CrossRef](#)]
41. Amjadi, O.; Tahmasebpoor, M. Improving fluidization behavior of cohesive Ca(OH)_2 adsorbent using hydrophilic silica nanoparticles: Parametric investigation. *Particuology* **2018**, *40*, 52–61. [[CrossRef](#)]
42. Amjadi, O.; Tahmasebpoor, M.; Aghdasinia, H. Fluidization behavior of cohesive Ca(OH)_2 powders mixed with hydrophobic silica nanoparticles. *Chem. Eng. Technol.* **2019**, *42*, 287–296. [[CrossRef](#)]
43. Gollsch, M.; Afflerbach, S.; Angadi, B.; Linder, M. Investigation of calcium hydroxide powder for thermochemical storage modified with nanostructured flow agents. *Sol. Energy* **2020**, *201*, 810–818. [[CrossRef](#)]
44. Castellanos, A.; Valverde, J.; Pérez, A.; Ramos, A.; Watson, P. Flow regimes in fine cohesive powders. *Phys. Rev. Lett.* **1999**, *82*, 1156–1159. [[CrossRef](#)]
45. Kariya, J.; Ryu, J.; Kato, Y. Development of thermal storage material using vermiculite and calcium hydroxide. *Appl. Therm. Eng.* **2016**, *94*, 186–192. [[CrossRef](#)]
46. Kariya, J.; Kato, Y. Development of thermal energy storage material using porous silicon carbide and calcium hydroxide. *Energy Procedia* **2017**, *131*, 395–406. [[CrossRef](#)]
47. Funayama, S.; Takasu, H.; Zamengo, M.; Kariya, J.; Kim, S.; Kato, Y. Composite material for high-temperature thermochemical energy storage using calcium hydroxide and ceramic foam. *Energy Storage* **2019**, *1*, e53. [[CrossRef](#)]
48. Funayama, S.; Takasu, H.; Kim, S.; Kato, Y. Thermochemical storage performance of a packed bed of calcium hydroxide composite with a silicon-based ceramic honeycomb support. *Energy* **2020**, *201*, 117673. [[CrossRef](#)]
49. Pan, Z.; Zhao, C. Prediction of the effective thermal conductivity of packed bed with micro-particles for thermochemical heat storage. *Sci. Bull.* **2017**, *62*, 256–265. [[CrossRef](#)]
50. Funayama, S.; Schmidt, M.; Mochizuki, K.; Linder, M.; Takasu, H.; Kato, Y. Calcium hydroxide and porous silicon-impregnated silicon carbide-based composites for thermochemical energy storage. *Appl. Therm. Eng.* **2023**, *220*, 119675. [[CrossRef](#)]

51. Fujii, I.; Tsuchiya, K.; Shikakura, Y.; Murthy, M. Consideration on thermal decomposition of calcium hydroxide pellets for energy storage. *J. Sol. Energy Eng.* **1989**, *111*, 245–250. [[CrossRef](#)]
52. Fujii, I.; Ishino, M.; Akiyama, S.; Murthy, M.; Rajanandam, K. Behavior of $\text{Ca}(\text{OH})_2/\text{CaO}$ pellet under dehydration and hydration. *Sol. Energy* **1994**, *53*, 329–341. [[CrossRef](#)]
53. Funayama, S.; Takasu, H.; Zamengo, M.; Kariya, J.; Kim, S.; Kato, Y. Performance of thermochemical energy storage of a packed bed of calcium hydroxide pellets. *Energy Storage* **2019**, *1*, e40. [[CrossRef](#)]
54. Gupta, A.; Armatis, P.; Sabharwall, P.; Fronk, B.; Utgikar, V. Kinetics of $\text{Ca}(\text{OH})_2$ decomposition in pure $\text{Ca}(\text{OH})_2$ and $\text{Ca}(\text{OH})_2\text{-CaTiO}_3$ composite pellets for application in thermochemical energy storage system. *Chem. Eng. Sci.* **2021**, *246*, 116986. [[CrossRef](#)]
55. Valverde-Pizarro, C.; Briones, L.; Sanz, E.; Escola, J.; Sanz, R.; González-Aguilar, J.; Romero, M. Coating of $\text{Ca}(\text{OH})_2/\gamma\text{-Al}_2\text{O}_3$ pellets with mesoporous Al_2O_3 and its application in thermochemical heat storage for CSP plants. *Renew. Energy* **2020**, *162*, 587–595. [[CrossRef](#)]
56. Cosquillo Mejia, A.; Afflerbach, S.; Linder, M.; Schmidt, M. Development of a moving bed reactor for thermochemical heat storage based on granulated $\text{Ca}(\text{OH})_2$. *Processes* **2022**, *10*, 1680. [[CrossRef](#)]
57. Briones, L.; Valverde-Pizarro, C.; Barras-García, I.; Tajuelo, C.; Sanz-Pérez, E.; Sanz, R.; Escola, J.; González-Aguilar, J.; Romero, M. Development of stable porous silica-coated $\text{Ca}(\text{OH})_2/\gamma\text{-Al}_2\text{O}_3$ pellets for dehydration/hydration cycles with application in thermochemical heat storage. *J. Energy Storage* **2022**, *51*, 104548. [[CrossRef](#)]
58. Criado, Y.; Alonso, M.; Abanades, J. Composite material for thermochemical energy storage using $\text{CaO}/\text{Ca}(\text{OH})_2$. *Ind. Eng. Chem. Res.* **2015**, *54*, 9314–9327. [[CrossRef](#)]
59. Criado, Y.; Alonso, M.; Abanades, J. Enhancement of a $\text{CaO}/\text{Ca}(\text{OH})_2$ based material for thermochemical energy storage. *Sol. Energy* **2016**, *135*, 800–809. [[CrossRef](#)]
60. Sakellariou, K.; Karagiannakis, G.; Criado, Y.; Konstandopoulos, A. Calcium oxide based materials for thermochemical heat storage in concentrated solar power plants. *Sol. Energy* **2015**, *122*, 215–230. [[CrossRef](#)]
61. Sakellariou, K.; Tsongidis, N.; Karagiannakis, G.; Konstandopoulos, A. Shortlisting of composite CaO -based structured bodies suitable for thermochemical heat storage with the $\text{CaO}/\text{Ca}(\text{OH})_2$ reaction scheme. *Energy Fuels* **2017**, *31*, 6548–6559. [[CrossRef](#)]
62. Sakellariou, K.; Criado, Y.; Tsongidis, N.; Karagiannakis, G.; Konstandopoulos, A. Multi-cyclic evaluation of composite CaO -based structured bodies for thermochemical heat storage via the $\text{CaO}/\text{Ca}(\text{OH})_2$ reaction scheme. *Sol. Energy* **2017**, *146*, 65–78. [[CrossRef](#)]
63. Xia, B.; Zhao, C.; Yan, J.; Khosa, A. Development of granular thermochemical heat storage composite based on calcium oxide. *Renew. Energy* **2020**, *147*, 969–978. [[CrossRef](#)]
64. Afflerbach, S.; Kappes, M.; Gipperich, A.; Trettin, R.; Krumm, W. Semipermeable encapsulation of calcium hydroxide for thermochemical heat storage solutions. *Sol. Energy* **2017**, *148*, 1–11. [[CrossRef](#)]
65. Afflerbach, S.; Afflerbach, K.; Trettin, R.; Krumm, W. Improvement of a semipermeable shell for encapsulation of calcium hydroxide for thermochemical heat storage solutions Material design and evaluation in laboratory and reactor scale. *Sol. Energy* **2021**, *217*, 208–222. [[CrossRef](#)]
66. Gollsch, M.; Afflerbach, S.; Drexler, M.; Linder, M. Structural integrity of calcium hydroxide granule bulks for thermochemical energy storage. *Sol. Energy* **2020**, *208*, 873–883. [[CrossRef](#)]
67. Cosquillo Mejia, A.; Afflerbach, S.; Linder, M.; Schmidt, M. Experimental analysis of encapsulated $\text{CaO}/\text{Ca}(\text{OH})_2$ granules as thermochemical storage in a novel moving bed reactor. *Appl. Therm. Eng.* **2020**, *169*, 114961. [[CrossRef](#)]
68. Guo, R.; Takasu, H.; Funayama, S.; Shinoda, Y.; Tajika, M.; Harada, T.; Kato, Y. Mechanical stability and heat transfer improvement of CaO -based composite pellets for thermochemical energy storage. *Chem. Eng. Sci.* **2022**, *255*, 117674. [[CrossRef](#)]
69. Bayon, A.; Bader, R.; Jafarian, M.; Fedunik-Hofman, L.; Sun, Y.; Hinkley, J.; Miller, S.; Lipinski, W. Techno-economic assessment of solid-gas thermochemical energy storage systems for solar thermal power applications. *Energy* **2018**, *149*, 473–484. [[CrossRef](#)]
70. Yan, J.; Zhao, C.; Pan, Z. The effect of CO_2 on $\text{Ca}(\text{OH})_2$ and $\text{Mg}(\text{OH})_2$ thermochemical heat storage systems. *Energy* **2017**, *124*, 114–123. [[CrossRef](#)]
71. Huang, C.; Xu, M.; Huai, X. Synthesis and performances evaluation of the spindle-shaped calcium hydroxide nanomaterials for thermochemical energy storage. *J. Nanopart. Res.* **2019**, *21*, 262. [[CrossRef](#)]
72. Bian, Z.; Li, Y.; Zhang, C.; Zhao, J.; Wang, Z.; Liu, W. $\text{CaO}/\text{Ca}(\text{OH})_2$ heat storage performance of hollow nanostructured CaO -based material from Ca -looping cycles for CO_2 capture. *Fuel Process. Technol.* **2021**, *217*, 106834. [[CrossRef](#)]
73. Li, Y.; Shi, J. Hollow-structured mesoporous materials: Chemical synthesis, functionalization and applications. *Adv. Mater.* **2014**, *26*, 3176–3205. [[CrossRef](#)]
74. Yuan, Y.; Li, Y.; Duan, L.; Liu, H.; Zhao, J.; Wang, Z. $\text{CaO}/\text{Ca}(\text{OH})_2$ thermochemical heat storage of carbide slag from calcium looping cycles for CO_2 capture. *Energy Convers. Manag.* **2018**, *174*, 8–19. [[CrossRef](#)]
75. Zhang, C.; Li, Y.; Bian, Z.; Zhang, W.; Wang, Z. Simultaneous CO_2 capture and thermochemical heat storage by modified carbide slag in coupled calcium looping and $\text{CaO}/\text{Ca}(\text{OH})_2$ cycles. *Chin. J. Chem. Eng.* **2021**, *36*, 76–85. [[CrossRef](#)]
76. Zhang, C.; Li, Y.; Yuan, Y.; Wang, Z.; Wang, T.; Lei, W. Simultaneous CO_2 capture and heat storage by a Ca/Mg -based composite in coupling calcium looping and $\text{CaO}/\text{Ca}(\text{OH})_2$ cycles using air as a heat transfer fluid. *React. Chem. Eng.* **2021**, *6*, 100–111. [[CrossRef](#)]
77. Feng, Y.; Deng, B.; Zhang, S.; Ding, Y.; Yang, X.; Zhang, M.; Yang, H. Basic characteristics of fast-reaction thermogravimetric analysis for kinetic studies of $\text{Ca}(\text{OH})_2/\text{CaO}$ fluidized thermochemical heat storage. *Clean Coal Technol.* **2022**, *28*, 1–10.

78. Feng, Y.; Huang, Z.; Bai, R.; Li, C.; Zhang, M.; Yang, H. Design and performance verification of a fast-reaction thermogravimetric analyzer. *Appl. Therm. Eng.* **2022**, *213*, 118783. [[CrossRef](#)]
79. Feng, Y.; Zhou, T.; Kong, H.; Bai, R.; Ding, Y.; Zhang, M.; Yang, H. Evaluation of thermodynamic and kinetic properties of carbide slag for fluidized thermochemical heat storage. *J. Energy Storage* **2022**, *56*, 105855. [[CrossRef](#)]

Disclaimer/Publisher's Note: The statements, opinions and data contained in all publications are solely those of the individual author(s) and contributor(s) and not of MDPI and/or the editor(s). MDPI and/or the editor(s) disclaim responsibility for any injury to people or property resulting from any ideas, methods, instructions or products referred to in the content.